

Observation of Neo-Classical Ion Pinch in the Electric Tokamak*

R. J. Taylor, T. A. Carter, J.-L. Gauvreau, P.-A. Gourdain, A. Grossman, D. J. LaFonteese, D. C. Pace, L. W. Schmitz, A. E. White, and T. F. Yates

Physics and Astronomy Dept., University of California, Los Angeles, CA 90095 U.S.A.

E-mail contact of main author: rtaylor@ucla.edu. Web: <http://et.ucla.edu>

* This research is supported by the U.S. Department of Energy grant DE-FG03-86ER53225

Abstract. A dominant particle pinch is observed in discharges of the Electric Tokamak (ET). As a result, the density increases dramatically, with the profile evolving in a self-similar manner. Due to density accumulation in the absence of significant core cooling, the Troyon limit ($\beta_N = I/aB \sim 3$) is reached in Ohmic plasmas in ET. The pinching rate is controlled with soft gas puffing. Hard puffing produces inverted density profiles that do not pinch due to MHD instabilities. The density threshold for pinching is $n(0) \sim 1 \times 10^{18} \text{ m}^{-3}$ in Ohmic discharges and $3 \times 10^{18} \text{ m}^{-3}$ in ICRF heated discharges. The ramp-up time of the density is typically 1 second. The ramps are terminated by internal disruptions due to beta collapse without any significant radiation loss. This collapse takes place mostly above the density limit ($n = 5 \times 10^{18} \text{ m}^{-3}$ with $B = 0.25 \text{ T}$ and $R = 5 \text{ m}$, $a = 1 \text{ m}$). The loop voltage remains low (0.4 V) during the ramp. In ICRF-heated discharges the ramps terminate at lower densities due to higher plasma temperatures. We observe no reduction in the electrostatic fluctuations. An analysis of the radial particle flux from equilibrium plasma profiles, based on Thomson data, is presented. It is found that the neoclassical “viscous” pinch (the old anomalous particle pinch) and the Ware pinch both contribute to the spontaneous density ramps and dominate neoclassical and anomalous (neo-Alcator like) particle diffusion for $r/a < 0.9$. We consider this pinch state H-mode like although it takes place without a core barrier, an edge transition, or fluctuation suppression.

1. Introduction

The Electric Tokamak was designed to take advantage of enhanced ion confinement due to negative plasma potential produced by fast ion orbit loss, classically. The negative radial potential for particle confinement was first proposed by Stix, who considered deep potential barriers induced by α -particle loss [1]. Stimulated ion trapping was observed in Macrotor during edge plasma bias experiments [2]. The inverse process produced by positive core bias, resulting in rapid plasma density loss, was also observed at that time. Additional improvements in electron heat confinement were expected due to size and low curvature. Enhanced confinement due to sheared poloidal rotation was considered only as a secondary goal with unpredictable results.

Extensive H-mode studies in CCT [3] confirmed the validity of these laminar “electric” effects. But unlike in ET, no regime of spontaneous high particle confinement time (τ_p) was found in CCT. Such a regime is characterized by an inward convection and a large $\tau_p / \tau_E (> 5)$ ratio. In general, enhanced particle confinement (H-mode) is also accompanied by improved heat confinement, usually limited to an H-factor less than two. In most cases this numerical factor can be easily attributed to changes in the radial particle convection. H-modes with the above properties have also been produced in ET by a biased electrode [4]. All these H-modes exhibit a strong bifurcation in poloidal flow in close numerical agreement with results from modified neo-classical theory [5].

In addition to edge H-modes and biased H-modes, a number of tokamaks have produced internal transport barrier (ITB) plasmas, for example, the ASDEX Upgrade tokamak [6]. Barrier formation is most commonly attributed to achieving a high shearing rate of the plasma flow and suppression of ion temperature gradient driven (ITG) turbulence.

In ET we observe a spontaneous density accumulation. The inward particle flow tends to dominate the anomalous radial diffusion, even in Ohmic plasmas, without a bifurcation event or ITB formation. Furthermore, this occurs without any measurable reduction in edge

turbulence, but requires the absence of low- m number MHD activity. The density evolution is characterized by the growth of a self-similar density profile, as seen in neo-Alcator type confinement regimes. In contrast to the neo-Alcator regime no neoclassical heat diffusion limit is reached, as there is no significant core plasma cooling. Instead the beta limit ($\beta_N \sim 3$) is reached even in Ohmic discharges. The density ramp-up-rate depends on edge plasma conditions for soft gas puffing. The pinch effect can be avoided by “over puffing”. In this case inverted density profiles are produced and exhibit persistent MHD instabilities.

In the remainder of the paper we will present the experimental results. These will be analyzed using the neoclassical pinch terms: the Ware pinch [7] and the neoclassical viscous pinch [8] (the electric field driven pinch in this paper). This pinch has also been called the “anomalous particle pinch”. The pinch term can dominate anomalous (turbulent) diffusion even for radial electric fields below the flow bifurcation threshold in ET. The results will be extrapolated to large tokamaks with higher toroidal field and lower aspect ratio. Conclusions drawn by Stix [1] for reactors with alpha particle sources will be retained even though these devices may reach bifurcated poloidal rotation.

2. Experimental Results

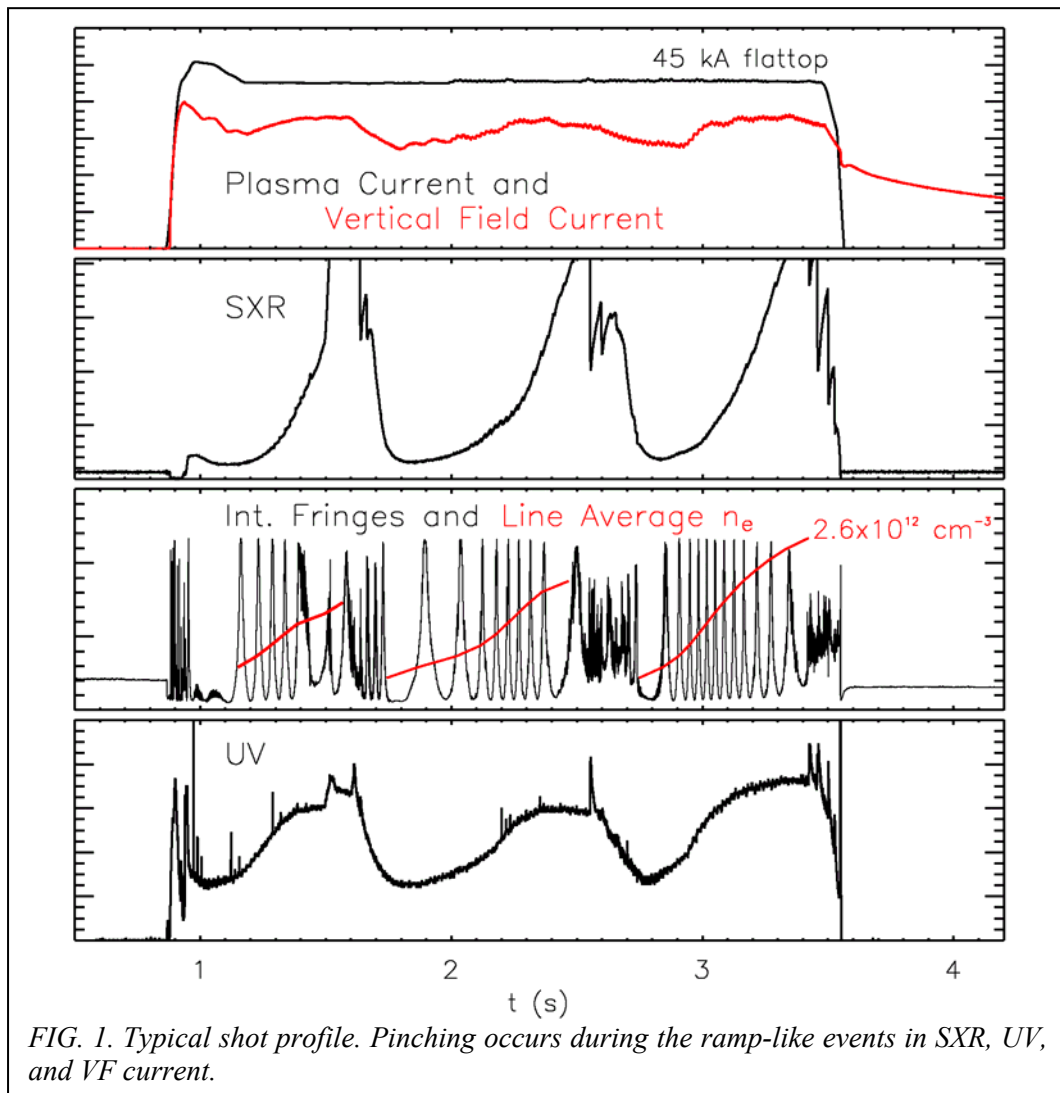


FIG. 1. Typical shot profile. Pinching occurs during the ramp-like events in SXR, UV, and VF current.

The pinch phenomenon is observed in the global data as shown in Figure 1. The rate of density rise, as observed from interferometry and Thomson scattering data (shown below), can be controlled by the rate of cold gas puffing at the plasma edge. The neutral ingestion radius is $r/a \sim 0.8$. For the data shown, the gas puff was held constant during the entire shot. In a 3 second period, 0 to 3 excursions can be obtained by adjusting the gas puffing. The increase in the vertical field current during the density ramps indicates increasing β . The comparison of the (central) SXR and UV emission indicates that there is no impurity accumulation. The density ramps are terminated by beta collapse, preceded by an increase of MHD activity, mostly above the density limit ($n_{DL}(0) = 10^{20}B/R = 5 \times 10^{18} \text{m}^{-3}$ with $B = 0.25\text{T}$ and $4\text{m} < R < 6\text{m}$). This MHD activity can be seen in the interferometer trace and in the Mirnov coil signals. The subsequent loss of plasma does not compromise the titanium gettered chamber walls. Consequently a sequence of density ramps can be produced with usually improving beta. Soft x-ray data, UV radiation data, interferometer data, Thomson profile data and edge probe data indicate that the ion trapping occurs in the core without the presence of sharp gradients.

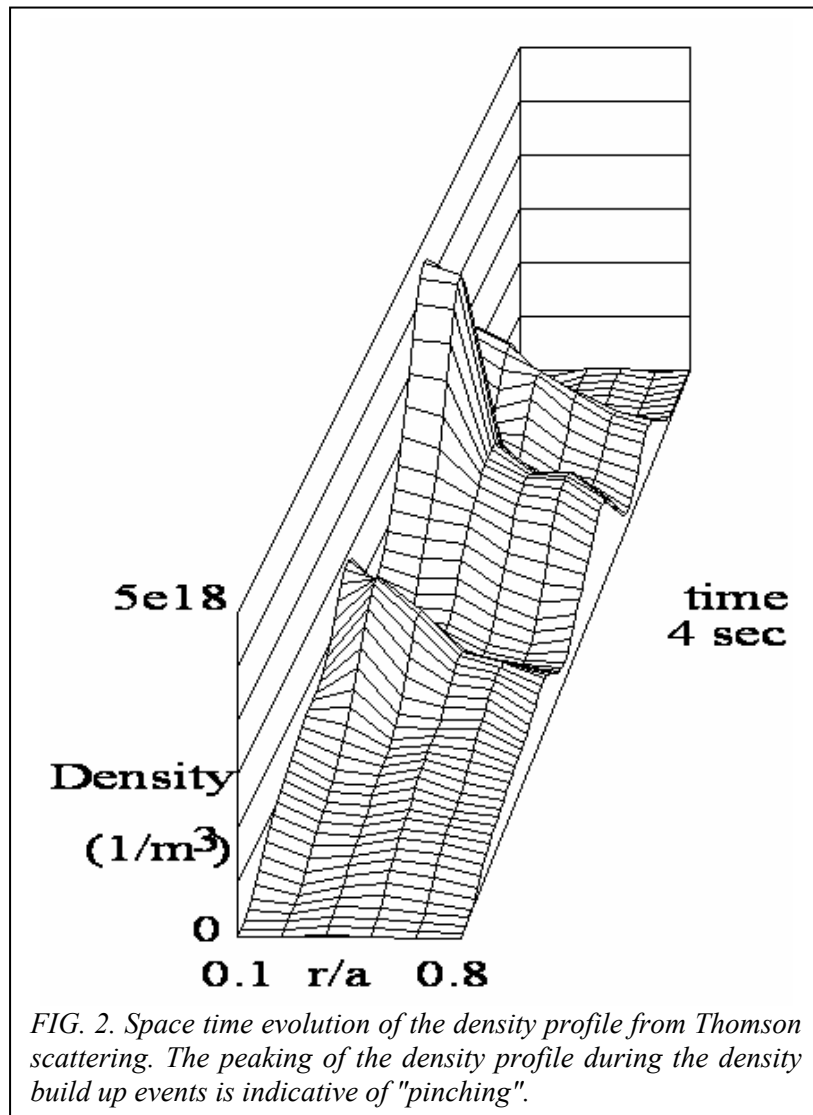


Figure 2 shows the evolution of the density profile (Thomson scattering) from $R = 5.1$ m to $R = 5.8$ m. In this shot there is some variation in self-similarity in favor of pinching. It is not clear if there is an internal barrier in the middle ramp. In the associated edge

measurements, the probe data indicate negative edge radial electric field E_r , which is observed consistently as shown in Figure 3. E_r is calculated using the measured floating potential and temperature according to $V_p = V_{fl} + 3.6 kT_e$. Here, V_p is the space potential and V_{fl} is the floating potential. As the accumulation proceeds, the electric field becomes less negative due to cooling. The swing to positive values occurs during beta collapse due to the plasma moving inwards as the probe samples the scrape-off layer with positive electric field for a short time period. The second event shows stronger negative E_r on the inner probe tips.

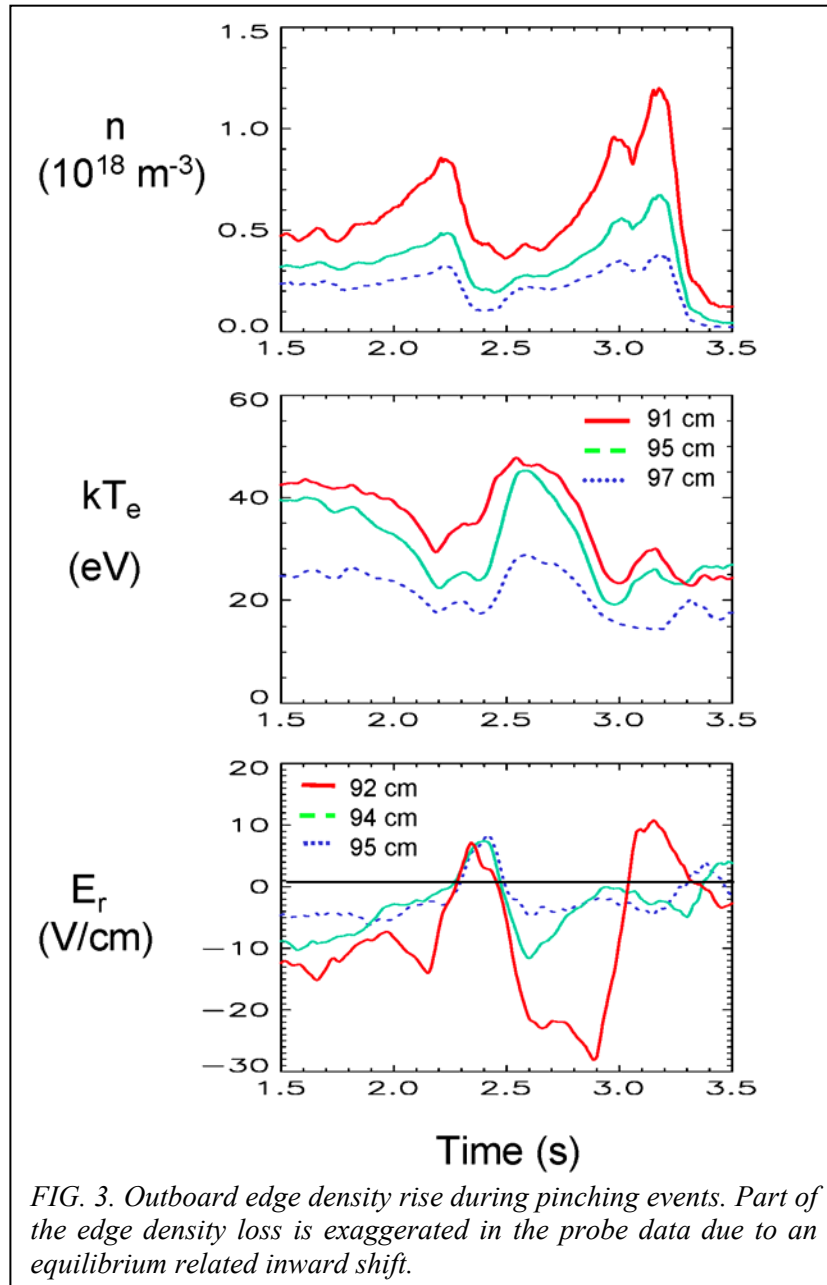
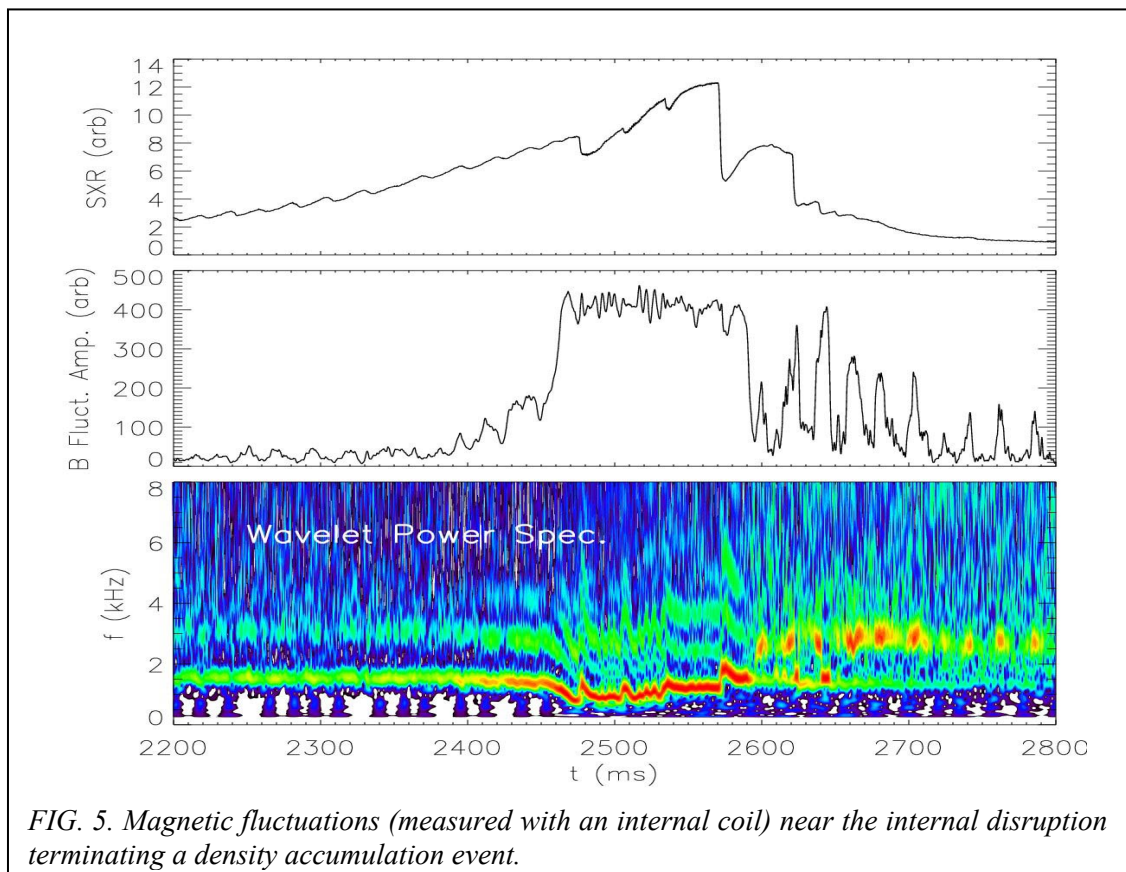
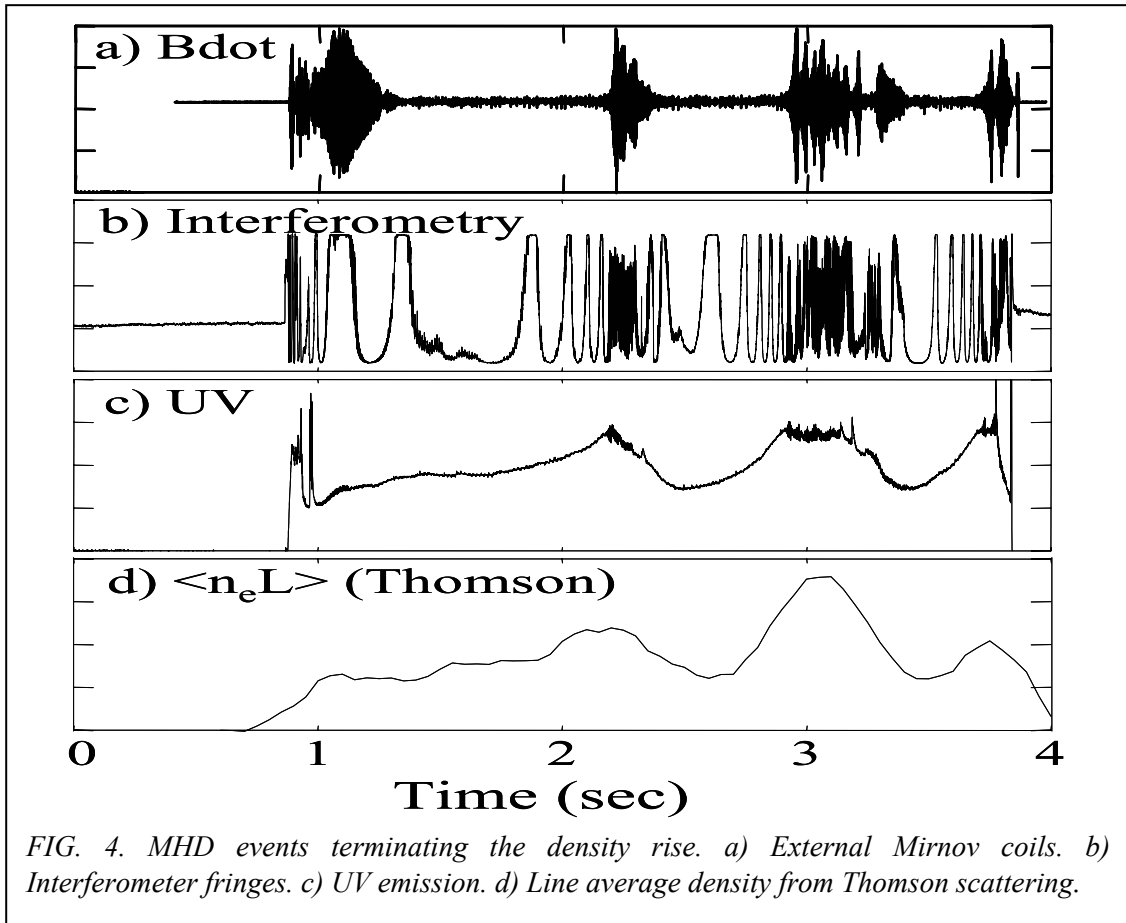


Figure 4 shows the effect of the MHD activity below 10 kHz on the Mirnov coils, on the UV signal and on the interferometry traces. A neoclassical tearing mode ($m/n = 2/1$) is observed to grow slowly as the density accumulation reaches its peak. Figure 5 shows the power spectrum and amplitude of magnetic fluctuations leading up to the internal disruption. In the disruption process, most of the plasma density is lost but the plasma current stays almost unperturbed.



3. Modeling and Analysis

Particle transport analysis efforts tend to consider the sources and “effective diffusivities” derived from power balance transport coefficients [9] without pinch terms. We will use an “ad hoc electric pinch term” and omit a detailed energy transport analysis.

The Ware pinch [7] will not be discussed in detail, instead we will focus more on the pinch term [8] related to the radial electric field. We will call this the “electric pinch” in this exposition.

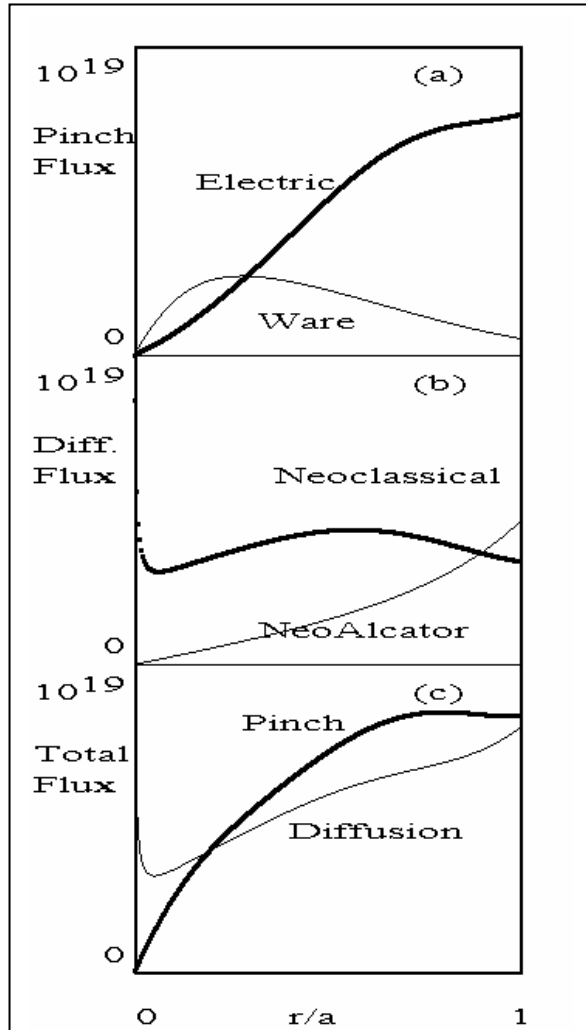


FIG. 6. Comparison of pinch fluxes (a), diffusion fluxes (b) and total fluxes (c). The pinch terms can dominate the diffusion terms. The unit of flux is $1/m^2/s$.

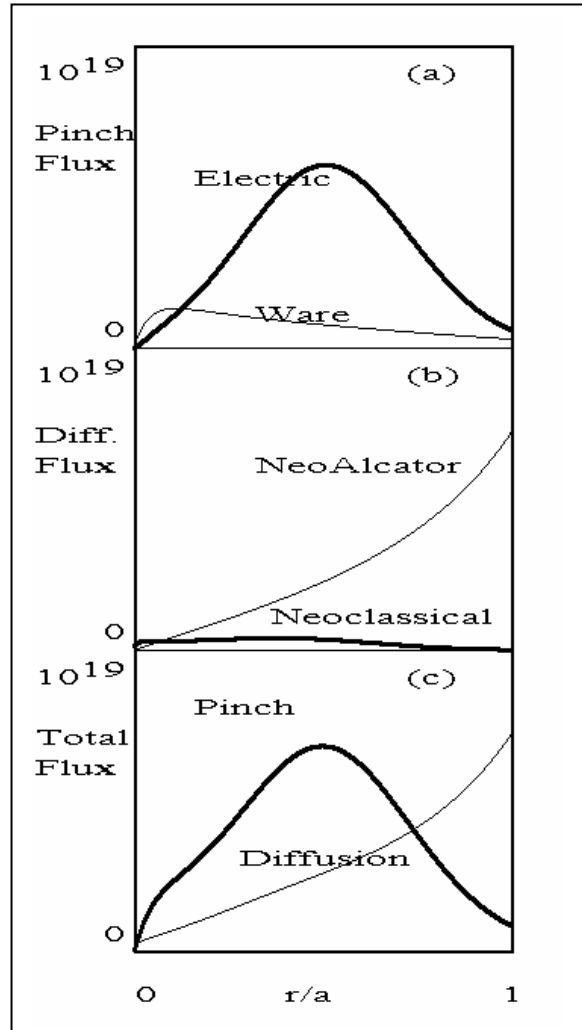


FIG 7. Electric pinch in ITER under alpha particle heating. Device potential of 0.5 MVolt was assumed. The unit of flux is $1/m^2/s$.

The radial particle influx can be estimated from the rate of density rise. For the neoclassical diffusion flux (Γ_{NC}), the Ware pinch (Γ_{Ware}) and “viscous” pinch (Γ_{pinch}) we use:

$$\Gamma_{NC-diff.}(r) = -\chi_{NC} \frac{dn(r)}{dr} \quad (1)$$

$$\Gamma_{ware}(r) = -\varepsilon^{1/2} \frac{n(r)}{(1+\nu_*)} \frac{V_{loop}}{2\pi R B_p} \quad (2)$$

$$\Gamma_{NC-pinch}(r) = -\chi_{NC} \frac{n(r)eE_r(r)}{kT_i(r)} \quad (3)$$

where, in the neoclassical pinch term, we used the neoclassical diffusivity for the various regimes of interest to represent mobility effects.

The anomalous particle diffusivity is estimated from the heat diffusivity and will be called the neo-Alcator diffusivity, even though this label is normally used to designate anomalous heat diffusivity or power balance diffusivity as in [6].

Figure 6 shows our estimates of the radial profiles of the inward flux due to the Ware pinch and the neoclassical “viscous electric pinch” along with the outward fluxes due to neoclassical diffusion and anomalous (neo-Alcator) diffusion.

Here we use reconstructed equilibrium profiles in ET for a high peak density shot ($n(0) = 5 \times 10^{12} \text{cm}^{-3}$) in the absence of toroidal rotation ($v_{\parallel} = 0$ by way of measurement). The neoclassical (electric) pinch dominates the inward flux for measured and estimated radial electric fields.

4. Reactor Relevance

Preliminary computations in Figure 7 for ITER indicate a significant pinch in the Ohmic mode (Ware). The reduction of the electric pinch in Ohmic ITER is due to its low aspect ratio (not show). However, the electric pinch will dominate particle fluxes if α particle heating is taken into account as shown.

5. Summary

In conclusion, we find that it will be essential to maintain a well-defined radial electric field in ET to control the viscous particle pinch. The pinch rate must be restricted to time scales consistent with the control of all equilibrium parameters (pressure gradient and current profile). A combination of external momentum sources and possible ergodisation of magnetic surfaces will be incorporated into the ET research program in order to achieve stationary plasma equilibrium in the future. Our experimental results, along with the theory result of Stix [1], suggest that a similar confinement excursion can occur in ITER under alpha particle transport condition if the radial electric field is not controlled. The control of the radial electric field (not including terms from toroidal rotation) will be difficult.

References

- [1] T. H. Stix, Phys. Rev. Lett. **24**, 135 (1970).
- [2] R. J. Taylor, L. Oren, Phys. Rev. Lett., **42** 446 (1979).
- [3] R. J. Taylor, M. Brown, B. Fried, *et. al.*, Phys. Rev. Lett. **63**, 2365 (1989).
- [4] R.J. Taylor, J.-L. Gauvreau, M. Gilmore, P.-A. Gourdain, D.J. LaFontese and L.W. Schmitz, Nucl. Fusion **42**, 46 (2002).
- [5] K. C. Shaing *et. al.*, Phys. Rev. Lett. **63**, 2370 (1989).
- [6] J. Stober, *et. al.*, Plasma Phys. Control. Fusion **44** A159 (2000)
- [7] A. A. Ware, Phys. Rev. Lett. **25**, 916 (1970)
- [8] Private conversation and K. C. Shaing, Phys. Rev. Lett. **86**, 640 (2001).
- [9] D. R. Baker, *et al.* Nucl. Fusion Vol. **40**. No. 5 1003 (2000).